Characterization of Supported Mn Species During the Preparation Process of Mn/SiO$_2$ Catalyst

Shohei Yamashita, Tomohiro Seigai, Yusaku Yamamoto,
Naoki Tsutsumi, Misaki Katayama, and Yasuhiro Inada
Department of Applied Chemistry, Graduate School of Life Sciences, Ritsumeikan University,
*1-1-1 Noji-Higashi, Kusatsu 525-*8577*, Japan*

Abstract

The chemical state of the Mn species was analyzed by means of the X-ray absorption fine structure (XAFS) spectroscopy for the Mn catalysts supported on SiO$_2$ prepared by the impregnation method using Mn(NO$_3$)$_2$·6H$_2$O, Mn(OAc)$_2$·4H$_2$O, and MnCl$_2$·4H$_2$O as the Mn(II) precursor salts. The *in-situ* XAFS measurements were carried out during the calcination process for the dried sample. For all cases, the initially impregnated species in the dried sample was commonly the Mn(II) hydrate with the respective anion. The finally formed Mn species was MnO$_2$ when the Mn(II) nitrate was used, whereas the Mn$_3$O$_4$ species was generated using the Mn(II) acetate and chloride salts. Because the coexisting nitrate ion can act as the oxidizing agent for the Mn(II) ion, the MnO$_2$ species was produced by accompanying the formation of NO$_2$ not only under the dilute O$_2$ atmosphere but also under the inert He atmosphere. The use of acetate and chloride as the precursor salt causes the formation of the Mn$_3$O$_4$ species on SiO$_2$ by the calcination procedure under the O$_2$ atmosphere. In this case, the oxidation of the Mn(II) species is driven by the molecular oxygen as the oxidizing agent existed in the gas phase. The much higher oxidation temperature (*ca.* 550 °C) for the chloride salt to form Mn$_3$O$_4$ than that (*ca.* 340 °C) for the acetate salt suggests the thermal stability of the anhydrous chloride species formed before the oxidation step.

1. Introduction

The supported metal catalysts are widely used for applications such as purification of harmful gas generated in industrial plants for the power generation. Many of the supported metal catalysts are used by loading a metal component, which is an active species, on the surface of thermally stable oxides such as SiO_2, Al_2O_3, CeO_2, etc. Catalysts using noble metals such as Pt and Rh are the mainstream in the chemical industry, however, because of their expensive costs, the base metal catalysts have attracted attention as the alternative material to the precious metals [1,2].

The catalyst in which the Mn species is supported on SiO_2 has a high activity for the oxidation reaction of volatile organic compounds (VOC) such as toluene and benzene [2-4]. A variety of stable oxides exist with the different oxidation state, such as MnO, Mn_3O_4, Mn_2O_3, and MnO_2, and the catalytic activity of the Mn catalyst is largely affected by the oxidation state of the active Mn species. For example, the selective catalytic reduction (SCR) of nitric oxide with ammonia is catalyzed by the MnO_2 species with the highest activity at low temperature, whereas the Mn_2O_3 species shows the highest selectivity for the same reaction [5,6]. Therefore, it is very important to understand the chemical state of the Mn species under the actual conditions of the catalysis reaction.

The chemical state of the supported Mn species is affected at the treatment procedure during its preparation process. It is know that the precursor salt of the Mn species is one important factor to change the chemical state. Is has been reported that the Mn_2O_3 species is generated after the calcination at 500 °C when Mn(II) acetate is used as the precursor salt, whereas the use of Mn(II) nitrate generates the MnO_2 species by the calcination at same temperature [5,7-11]. Such aspects have been empirically known and used to control the supported Mn species, however, the origin to change the supported Mn species is not sufficiently understood, and thus the active control of the supported Mn species is impossible for the sophisticated utilization of the chemical state difference.

In this study, we have synthesized the supported Mn catalysts using various Mn precursor salts by the impregnation method, and *in-situ* XAFS technique has been applied to analyze the Mn species during their preparation process, *i.e.*, the heating process under dilute O_2 atmosphere up to *ca.* 700 °C. It has been aimed to clarify the mechanism to change the chemical state of the supported Mn species on SiO_2.

2. Experimental

2.1. Catalyst preparation

The Mn catalysts were prepared by the impregnation method using SiO_2 (JRC-SIO-10) distributed by the Catalysis Society of Japan with the Mn loading of 10 wt%. Manganese(II) nitrate hexahydrate ($Mn(NO_3)_2\cdot 6H_2O$), manganese(II) acetate tetrahydrate ($Mn(CH_3CO_2)_2\cdot$

$4H_2O$), and manganese(II) chloride tetrahydrate ($MnCl_2\cdot4H_2O$) were used as the Mn precursor salt. An adequate amount of the Mn precursor salt was dissolved in deionized water, and the powder of SiO_2 was added into the solution. The mixture was stirred for 1 h, and the suspension was dried at 60 °C for 60 h. The obtained powder was calcined in air for 2 h. Totally 6 catalysts were prepared by changing the calcination temperature at 100 °C, 200 °C, 300 °C, 400 °C, 500 °C, and 600 °C for each precursor salt.

2.2. XAFS measurement and characterization

The transmission XAFS measurements at the Mn K edge were carried out at the BL-3 station of the SR Center (Ritsumeikan University) and at the BL-9C and -12C stations at the Photon Factory (KEK). The higher-order harmonics in the incident X-ray was suppressed by detuning the double-crystal monochromator at the latter stations. The heating process was subjected by the *in-situ* XAFS measurements for the dried sample in which the Mn precursor compound was impregnated. The temperature was raised up to 700 °C at the increasing rate of 10 °C/min under the O_2 atmosphere diluted by He (10 vol%) with the flow rate of 200 cm^3/min. In addition to the XAFS measurements, the X-ray diffraction (XRD) and the thermogravimetric measurements with the differential thermal analysis (TG-DTA) were performed to characterize the supported Mn species.

3. Results and discussion

3.1. Chemical state change for the Mn(II) nitrate precursor

Figure 1 shows the XANES spectrum, the EXAFS oscillation function, and the Fourier transform function for the dried sample, in which the Mn(II) nitrate precursor was impregnated. The corresponding data for the 0.5 M aqueous solution of the Mn(II) nitrate salt are given in

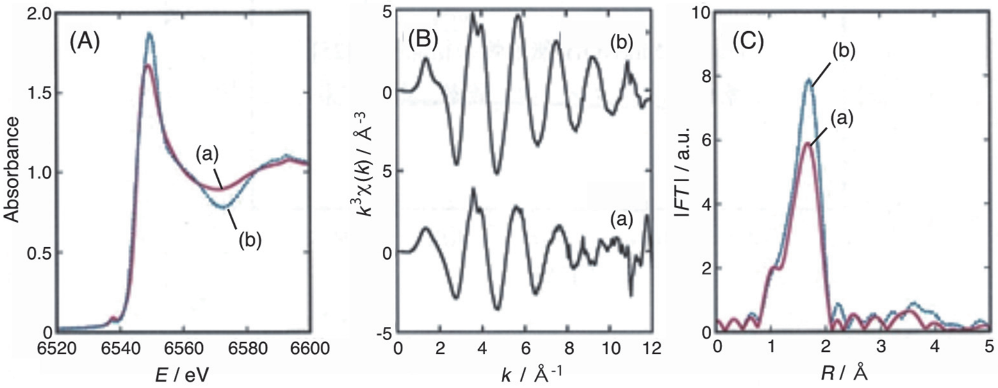

Fig. 1. The XANES spectrum (A), the EXAFS oscillation function (B), and the Fourier transform (C) are shown for the dried sample using the $Mn(NO_3)_2\cdot6H_2O$ precursor (a) and the 0.5 M aqueous solution of $Mn(NO_3)_2$ (b).

Fig. 1 for comparison. All data are almost comparable, and it is thus concluded that the Mn(II) hydrate exists on SiO_2 by accompanying the nitrate counter ion. Although the absorption edge and the overall EXAFS feature are similar for both samples, it is obvious that the white line intensity and the Fourier transform magnitude for the nearest Mn–O interaction observed at around 1.8 Å are low for the dried catalyst sample. The EXAFS analysis revealed that the average coordination number of the Mn–O interaction was 4.6 ± 0.2 and its bond distance was 2.18 ± 0.02 Å. The Mn–O distance is in agreement with that of the 6-coordinate Mn(II) hydrate [12], whereas the impregnated Mn(II) nitrate reduces the coordination number to *ca.* 5, indicating the direct coordination of the nitrate ion and/or the participation of the surface O atom of SiO_2 in the first coordination shell of the Mn(II) ion. The former contributes to neutralize the positive charge of the Mn(II) center, and the latter acts as the bulky ligand.

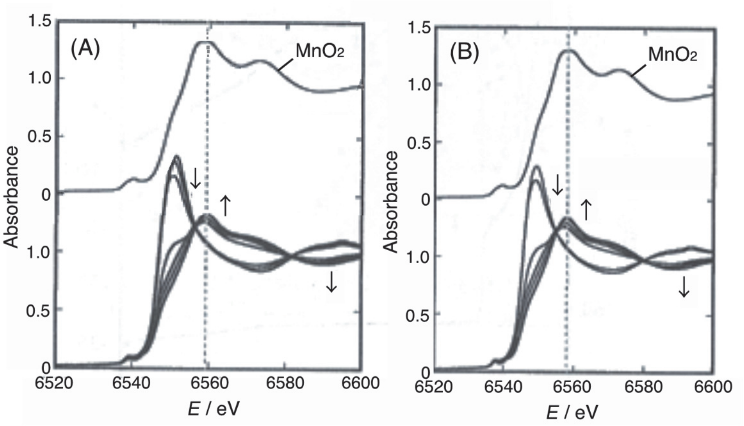

Fig. 2. XANES spectral change during the heating process of the dried samples under the diluted O_2 atmosphere (A) and under the pure He atmosphere (B). The spectrum of MnO_2 is indicated for comparison.

The XANES spectral change is shown in Fig. 2 for the heating process of the dried sample under the dilute O_2 atmosphere. The corresponding XANES change under the pure He atmosphere without O_2 is compared in Fig. 2. The white line intensity was slightly reduced at the temperature range below 100 °C, and its drastic decrease was observed at *ca*. 200 °C together with the shift of the white line peak to the higher energy for both conditions. The final energy of the white line peak was almost identical to that of the reference MnO_2 powder. It is thus concluded that the Mn(II) nitrate precursor is oxidized to the Mn oxide with the valence of +4 during the calcination process. The same oxidation reaction was also taken place in an inert He atmosphere. The same conversion temperature observed for both conditions strongly indicate that the oxidizing agent of the Mn(II) nitrate precursor is not the molecular oxygen in the gas phase but the nitrate ion in the impregnated precursor salt.

The present EXAFS measurements clearly demonstrated that the Fourier transform functions below 200 °C were almost consistent with that of the aqueous solution of Mn(II) ion, while the second neighboring interaction peak at *ca.* 2.2 Å, which is characteristic to the Fourier transform function of MnO_2, appeared at above 200 °C. The oxidation from Mn(II) nitrate to MnO_2 is clearly supported by the drastic change of XANES and EXAFS observed at around

200 °C for both conditions. The slight decrease of the white line intensity at lower temperature rage is ascribed by the release of the bound water molecules, which leads the decrease in symmetry around the Mn(II) center. Nohman *et al.* have reported that two water molecules are released from $Mn(NO_3)_2{\cdot}4H_2O$ to form $Mn(NO_3)_2{\cdot}2H_2O$ at 135 °C and the anhydrate $Mn(NO_3)_2$ salt is generated by the further dissociation of two water molecules at *ca.* 175 °C [13]. The present study clarified that the formed anhydrous Mn(II) nitrate was converted to MnO_2 by equation (1) at around 200 °C on SiO_2 by the self conversion reaction without any additional oxidizing reagents.

$$\mathrm{Mn(NO_3)_2} \quad \rightarrow \quad \mathrm{MnO_2 + 2NO_2} \tag{1}$$

The present results are consistent with the formation of MnO_2 and NO_2 from $Mn(NO_3)_2{\cdot}4H_2O$ on Al_2O_3 reported by Malecka *et al.* [14]. The same reaction observed in an inert condition strongly demonstrates the function of nitrate ion as the oxidizing agent.

3.2. Chemical state change for the Mn(II) acetate precursor

The XANES spectrum, the EXAFS oscillation function, and the Fourier transform function of the dried sample, in which the Mn(II) acetate precursor is impregnated, are compared with those of the Mn(II) aqueous solution in Fig. 3. All data are almost comparable, and it is thus considered that the Mn(II) acetate hydrate exists on SiO_2. The EXAFS analysis revealed that the average coordination number of the Mn–O interaction was 4.7 ± 0.2 and its bond distance was 2.14 ± 0.08 Å and that the 5-coordinate Mn(II) acetate hydrate was formed after the drying process similar to the case of the Mn(II) nitrate described above. According to the reported crystal structure for $Mn(CH_3CO_2)_2{\cdot}4H_2O$ and $Mn(CH_3CO_2)_2{\cdot}2H_2O$ [15,16], in which both the water and acetate molecules coexist in the first coordination shell of the Mn(II) ion, the Mn–O(water) bond distance of 2.15–2.17 Å is shorter than the Mn–O(acetate) bond distance of 2.22–2.23 Å. However, the difference is not enough to distinguish as the double peak in the

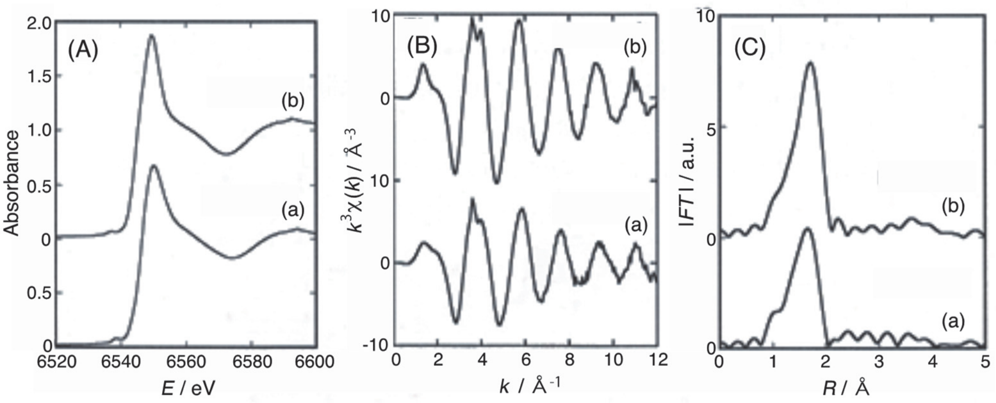

Fig. 3. The XANES spectrum (A), the EXAFS oscillation function (B), and the Fourier transform (C) are shown for the dried sample using the $Mn(OAc)_2{\cdot}4H_2O$ precursor (a) and the 0.5 M aqueous solution of $Mn(NO_3)_2$ (b).

Fourier transform function. A slight broaden Mn–O interaction for the dried sample may indicate such the structural disorder.

Figure 4 shows the XANES spectral change for the heating process of the dried sample under the O_2 and He atmosphere. The chemical conversion from Mn(II) acetate to the Mn oxide was clearly suggested by the XANES change observed under the dilute O_2 atmosphere (see Fig. 4(A)). The gradual drop of the white line peak intensity was observed up to *ca.* 320 °C, and the peak energy drastically shifted at around 340 °C. The X-ray energy of the shifted white line peak was consistent with that of the Mn_3O_4 powder, and thus the formed species was assigned as Mn_3O_4 supported on SiO_2 when the Mn(II) acetate precursor was used. The smooth feature of the observed XANES spectrum compared with that of the Mn_3O_4 powder is considered to be due to the small particle size of Mn_3O_4 supported on SiO_2. It is marked contrast that such the higher energy shift of the white line peak was not observed in the case of the He atmosphere up to 700 °C.

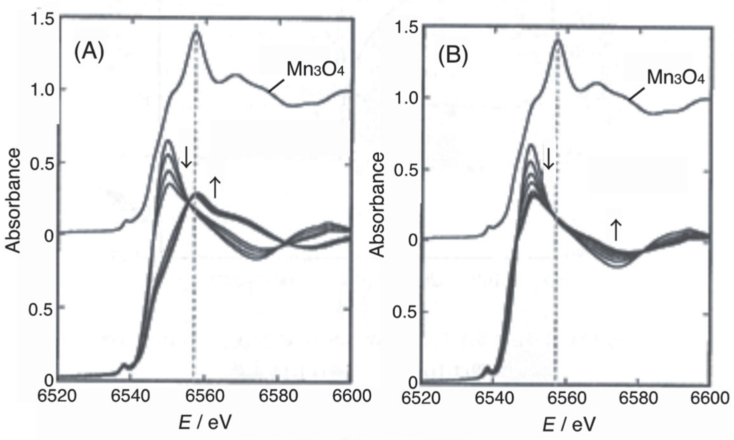

Fig. 4. XANES spectral change during the heating process of the dried samples under the diluted O_2 atmosphere (A) and under the pure He atmosphere (B). The spectrum of Mn_3O_4 is indicated for comparison.

The X-ray absorbance change at 6550 eV, which corresponds to the white line peak energy of the initial Mn(II) acetate hydrate, is plotted as a function of temperature in Fig. 5. The gradual decrease at the temperature range below 340 °C under the dilute O_2 atmosphere was in agreement with that observed in the He atmosphere. The EXAFS analysis at this temperature range reveled that the average coordination number and the bond distance of the nearest Mn–O interaction was decreased from 4.7 to 3.3 and from 2.14

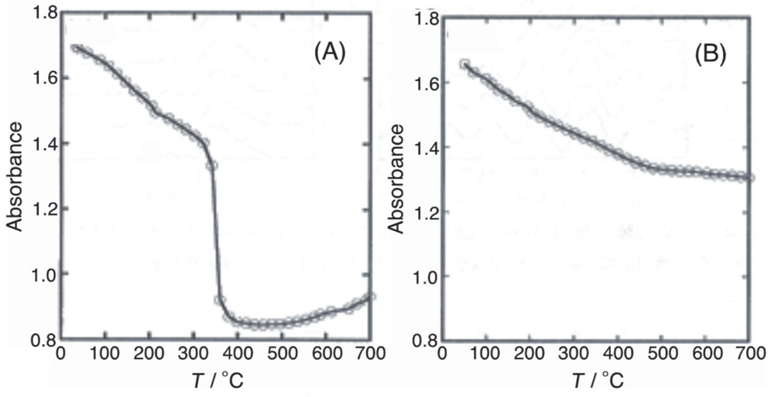

Fig. 5. The change of X-ray absorbance at 6550 eV as a function of temperature during the heating process of the dried samples under the diluted O_2 atmosphere (A) and under the pure He atmosphere (B).

to 2.07 Å, respectively. The observed change in the structure parameters indicates the dissociation of the hydrate water molecules as observed for the Mn(II) nitrate precursor at the temperature range below 200 °C. This consideration is supported by the drastic change of the structure parameters at above 340 °C, where the average coordination number is increased to 4.8 and the bond distance is shortened to 1.92 Å. These values are almost consistent with the corresponding values of 5 and 1.89 Å for Mn_3O_4, indicating that the Mn(II) acetate is oxidized to Mn_3O_4 at around 340 °C. Furthermore, the TG-DTA data showed the exothermic weight loss at around 320 °C, and the XRD pattern of Mn_3O_4 was appeared for the sample calcined above 400 °C.

In contrast to the results under the dilute O_2 atmosphere, the conversion to Mn_3O_4 was not observed under the He atmosphere as seen in Fig. 4(B). Only the decrease in the average coordination number and the bond distance of the nearest Mn–O interaction was observed in the present temperature range, and the values reached to 2.7 ± 0.4 and 2.07 ± 0.04 Å at elevated temperatures under the He atmosphere, respectively. These values are almost comparable to those observed at 300 °C before the conversion to Mn_3O_4 under the dilute O_2 atmosphere. It is thus clearly indicated that the oxidation of the Mn(II) acetate to generate the Mn_3O_4 species is driven by the molecular oxygen as the oxidizing agent in the gas phase. The oxidation to Mn_3O_4 proceeded at around 320 °C also supports that the oxidation to MnO_2 proceeded at *ca.* 200 °C in the case of the Mn(II) nitrate precursor is driven by the nitrate ion.

3.3. Chemical state change for the Mn(II) chloride precursor

Figure 6 shows the XANES spectrum, the EXAFS oscillation function, and the Fourier transform function of the dried sample, in which the Mn(II) chloride precursor was impregnated. The main peak observed in the Fourier transform function was successfully analyzed by assuming two scattering shells of the Mn–O and Mn–Cl interactions. The optimized values of

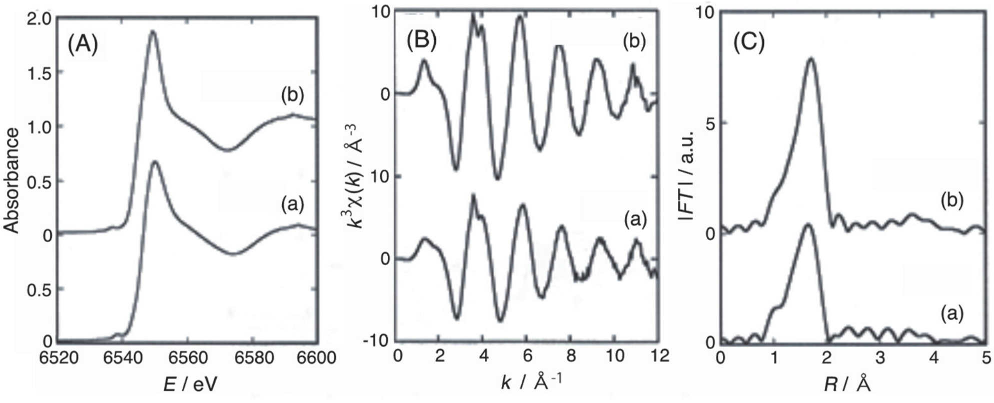

Fig. 6. The XANES spectrum (A), the EXAFS oscillation function (B), and the Fourier transform (C) are shown for the dried sample using the $MnCl_2 \cdot 4H_2O$ precursor (a) and the 0.5 M aqueous solution of $Mn(NO_3)_2$ (b).

the structure parameters are as follows: the average coordination number and the bond distance are 3.0 ± 1.8 and 2.13 ± 0.08 Å, respectively, for the Mn–O interaction and are 2.8 ± 1.5 and 2.53 ± 0.11 Å, respectively, for the Mn–Cl interaction. These bond distances are in accordance with those reported for the crystal structure of $MnCl_2 \cdot 4H_2O$ and $MnCl_2 \cdot 2H_2O$ [17,18]. It is thus concluded that *ca.* 3 water molecules and 3 chloride ions coordinate to the Mn(II) ion to form the octahedral Mn(II) chloride hydrate on SiO_2.

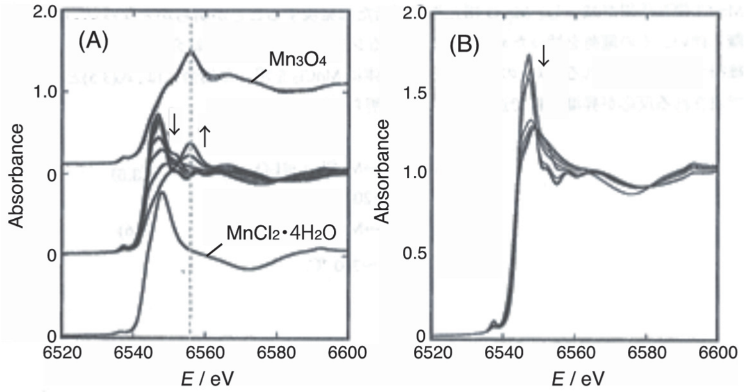

Fig. 7. XANES spectral change during the heating process of the dried samples under the diluted O_2 atmosphere (A) and under the pure He atmosphere (B). The spectra of Mn_3O_4 and $MnCl_2 \cdot 4H_2O$ are indicated for comparison.

The observed XANES change during the heating process under the dilute O_2 atmosphere is compared in Fig. 7 with that observed under the He atmosphere. For the latter case, the white line peak intensity was dropped without the apparent energy shift of the absorption edge. The EXAFS oscillation function of the spectra at around 350 °C were well reproduced by the single Mn–Cl interaction, and the optimized Mn–Cl bond distance of 2.51 ± 0.01 Å was consistent with that in the anhydrous $MnCl_2$ crystal [18]. The bound water molecules are thoroughly released during the heating process up to *ca.* 200 °C under the He atmosphere. The similar XANES change was also observed under the dilute O_2 atmosphere in the temperature range up to *ca.* 350 °C, whereas the white line peak was obviously shifted to the higher energy at much higher temperatures around 550 °C and its peak top energy was finally matched to that of the Mn_3O_4 powder (see Fig. 7(A)). The second neighboring interaction peak at *ca.* 2.3 Å observed in the Fourier transform function, which is characteristic to the Mn_3O_4 species, was observed at above 550 °C, and the average coordination number and the bond distance for the nearest Mn–O interaction was finally changed to 4.6 ± 0.8 and 1.90 ± 0.02 Å, respectively, at 700 °C. These are in agreement with the values for Mn_3O_4, indicating that the Mn(II) chloride is oxidized to Mn_3O_4 at above 550 °C by the molecular oxygen existed in the atmosphere. It should be noted that the oxidation temperature (*ca.* 550 °C) of the Mn(II) chloride salt to form Mn_3O_4 is much higher than the corresponding temperature (*ca.* 340 °C) of the Mn(II) acetate salt although the same Mn_3O_4 species is formed on SiO_2, suggesting the thermal stability of the anhydrous Mn(II) chloride species.

4. Conclusion

This study has clearly revealed that the chemical state of the supported Mn species is seriously affected by the property of the precursor salt used as the Mn source. The nitrate ion with the oxidizing ability generates the MnO_2 species, and the oxidation reaction of the impregnated Mn(II) nitrate proceeds at around 200 °C on SiO_2 by the self conversion reaction without any additional oxidizing reagents. Thus, the formation of MnO_2 is possible by the heating treatment even in the inert He atmosphere. On the other hand, the spinel oxide compound, Mn_3O_4, is generated by the calcination treatment for the impregnated Mn(II) acetate and chloride. The molecular oxygen in the atmosphere is necessary to oxidize the Mn(II) species for both cases. The formation temperature of the Mn_3O_4 species on SiO_2 is *ca.* 340 °C for the Mn(II) acetate, while the calcination at much higher temperature at *ca.* 550 °C is necessary in the case of the Mn(II) chloride. The *in-situ* XAFS measurements revealed that the anhydrous Mn(II) acetate or chloride was existed before the conversion to Mn_3O_4. The aspects about the chemical state of the supported Mn species obtained in this study are important and useful for preparing the desired active Mn species to control the catalytic performance.

Acknowledgment

The XAFS measurements at the Photon Factory (KEK) have been performed under the approval of the Photon Factory Program Advisory Committee (Proposal No. 2015G544).

Reference

[1] J. Li, X. Liang, S. Xu, and J. Hao, *Appl. Catal. B*, **90**, 307 (2009).
[2] J. Lou, H. W. Yang, and C. H. Lin, *Aerosol Air Qual. Res.*, **9**, 435 (2009).
[3] H. Einaga, S. Yamamoto, N. Maeda, and Y. Teraoka, *Catal. Today*, **242**, 287 (2014).
[4] H. Einaga and A. Ogata, *J. Hazard. Mater.*, **164**, 1236 (2009).
[5] F. Kapteijn, L. Sigoredjo, and A. Andreini, *Appl. Catal. B*, **3**, 173 (1994).
[6] J. Li, H. Chang, L. Ma, J. Hao, and R. T. Yang, *Catal. Today*, **147**, 175 (2011).
[7] M. Jin, J. H. Kim, L. Ma, J. Jeon, J. Jongsoo, G. N. Bae, and Y. K. Park, *Catal. Today*, **204**, 108 (2013).
[8] E. Park, M. Kim, H. Jung, S. Chin, and J. Jung, *ACS Catal.*, **3**, 1518 (2013).
[9] J. Li, J. Chen, R. Ke, C. Luo, and J. Hao, *Catal. Commun.*, **8**, 1896 (2007).
[10] C. Sun, Y. Tang, F. Gao, J. Sun, K. Ma, C. Tang, and L. Dong, *Phys. Chem. Chem. Phys.*, **17**, 15996 (2015).
[11] J. H. Ko, S. H. Park, J. K. Jeon, S. S. Kim, S. C. Kim, J. M. Kim, D. Chang, and Y. K. Park, *Catal. Today*, **185**, 290 (2012).
[12] H. Ohtaki and T. Radnai, *Chem. Rev.*, **93**, 1157 (1993).

[13] A. K. H. Nohman, H. M. Ismail, and G. A. M. Husseim, *J. Anal. Appl. Pyro.*, **34**, 256 (1995).

[14] B. Malecka, A. Lacz, E. Drozdz, and A. Makecki, *J. Therm. Anal. Calorim.*, **119**, 1053 (2015).

[15] S. Y. Li, Y. H. Li, H. L. Liu, H. L. Zhu, and D. Q. Wang, *Crystallogr. New Crystal Struct.*, **218**, 319 (2003).

[16] C. Y. Cheng and S. L. Wang, *Acta Cryst.*, *C*, **47**, 1734 (1991).

[17] B. Morosin and E. J. Graeber, *J. Chem. Phys.*, **42**, 898 (1965).

[18] R. W. G. Wyckoff, *Crystal Struct.*, **1**, 239 (1963).